멤브레인(Membrane Journal)
Vol. 15, No. 2 June, 2005, 175-186

염수의 탈염을 위한 전기투석 농축실에서의 스케일 형성

양 정 훈 · 연 경 호 · 문 승 현†

광주과학기술원 환경공학과

(2005년 5월 24일 접수, 2005년 6월 21일 채택)

Scale Formation in the Concentrate Compartment of an Electrodialysis Stack During Desalination of Brackish Water

Jung-Hoon Yang, Kyeong-Ho Yeon, and Seung-Hyeon Moon†

Department of Environmental Science and Engineering, Gwangju Institute of Science and Technology (GIST), 1 Oryong-dong, Buk-gu, Gwangju 500-712, Korea

(Received May 24, 2005, Accepted June 21, 2005)

요 약: 전기투석 공정에서 이온교환막 표면에 형성되는 스케일 영향을 조사하기 위해 장기간 동안 운전되었다. 탈염공정 동안, Ca^{2+}과 SO_4^{2-} 이온의 농도는 농축실에서 연속적으로 증가하였으며 양이온교환막(Neosepta CMX)표면에 침전이 발생하였다. 초기 스케일 형성동안, 공정성능과 막 특성의 변화는 농축실 염농도 증가에 기인하여 일어나는 양이온교환막의 한계전류밀도가 감소하는 것을 제외하곤 미미하였다. 공정운전이 진행됨에 따라 양이온교환막의 한계전류밀도는 물의 해리현상이 진행되어 300 A/m^{2}까지 감소하였다. 막 오염은 농축실에서 양이온교환막 표면에 형성된 스케일과 물의 해리현상에 의해 유발된다는 결론을 얻었으며, 이러한 스케일 형성은 $CaSO_4$의 용해도에 의해 예측 가능한 것을 알 수 있었다.

Abstract: An electrodialysis process was operated for a long period to investigate the scale formation on the membrane surface. During the desalination process, concentration of Ca^{2+} and SO_4^{2-} ions increased continuously in the concentrate compartment and eventually caused precipitation on the cation exchange membrane (Neosepta CMX) surface. During the initial scale formation, the performance of the process and membrane characteristics did not show significant changes, except the decrease in limiting current density of the CMX membrane occurring due to increase in the salt concentration in the concentrate compartment. Eventually, the limiting current density of the fouled CMX membrane dropped significantly to 300 A/m^2 as water dissociation occurred in the CMX membrane. It was concluded that the fouling was caused mainly by the scale formation on the cation exchange membrane surface in the concentrate and consequent water dissociation. Also the scale formation was reasonably predicted by the solubility of $CaSO_4$.

Keywords: *electrodialysis, scale, limiting current density, back diffusion, water dissociation*

1. Introduction

Electrodialysis is an electrochemical process for the separation of ions from one solution to another, under the influence of electrical potential difference across charged membranes[1-5]. This process has been widely applied in the treatment of brackish water for potable use or to desalt and concentrate effluents for the reuse. Despite the fact that electrodialysis is a well proven technology with a multitude of systems operating worldwide, its share in brackish water desalination is very small in contrast to reverse osmosis or thermal methods[6-10].

The wide application of electrodialysis for demineralization of naturally diluate solutions has been restricted until recently for a number of reasons, such

†주저자(e-mail : shmoon@gist.ac.kr)

as a risk of forming deposits consisting of insoluble salts in the concentrate and desalination chambers, the high electrical resistance of solution and a low flux of the ions to be removed through the membranes[11-17]. Desalination of the waters containing a considerable amount of calcium ion, such as brackish water, is accompanied by the deposition of fairly insoluble compounds on the membranes. This phenomenon occurs during both pressure-driven membrane and electro-membrane processes, and is usually referred to as membrane scaling. If scaling, such as $CaSO_4$ deposition, occurs on the membrane surface when treating hard waters, this scale is often removed by combined methods, but their use is both expensive and laborious[18].

Therefore, it is meaningful to identify the conditions under which the scale is formed and the effect of the scale on an electrodialysis process. In this study, we have investigated the effect of insoluble salts on the process efficiency for a long-period electrodialysis operation to desalinate brackish water by using an automatic electrodialysis system. Furthermore, some phenomena following the formation of scale layers on the membrane surface were observed and analyzed. The influences caused by concentration differences between the diluate and the concentrate solutions also were investigated by continuously concentrating the concentrate solution, *i.e.*, with uncontrolled concentrate stream.

2. Experimental

2.1. Materials

In this experiment, Neosepta CMX (Tokuyama Co., Japan) cation-exchange membrane and Neosepta AMX (Tokuyama Co., Japan) anion-exchange membrane were used. The Neosepta CMX and AMX membranes contain sulfonic acid groups and ammonium groups as fixed charges, respectively. These are reinforced and standard grade membranes for general concentration ranges or desalination purposes[19].

The brackish water was prepared using NaCl, Na_2SO_4, KCl, $NaHCO_3$, $MgCl_2 \cdot 6H_2O$, $CaCl_2 \cdot 2H_2O$ and distilled water. This solution had the same composition as sea water, but the salt concentration was 10‰; 112 mM NaCl, 8.00 mM Na_2SO_4, 2.86 mM KCl, 0.572 mM $NaHCO_3$, 24.8 mM $MgCl_2 \cdot 6H_2O$, 3.26 mM $CaCl_2 \cdot 2H_2O$. As an electrode rinse solution, 0.5 M Na_2SO_4 solution was used.

2.2. Current-voltage Measurements

The relationship of current and voltage was analyzed under the two different conditions.

2.2.1. Current-voltage Relation for the Same Salt Concentration in the Concentrate and Diluate Compartments

Each of the current-voltage curves for the CMX and AMX membranes was obtained using an electrodialysis stack as shown in Fig. 1. This stack had a two cell-pair configuration and each cell-pair consisted of alternating AMX and CMX membranes. The effective area of each membrane was 100 cm^2.

The brackish water had only one channel that flowed through the diluate compartment and the concentrate compartment. The two solutions of the two compartments were well mixed in the storage tank so that the concentration in both compartments did not change even after potential was applied to the stack.

Current-voltage curves were obtained by a stepwise increase in the current and the measurement of resulting potential. After the current was increased, which was done every 5 min, the electrical potential difference across the membrane was measured with a multimeter (HP 34401, USA) every two seconds. The average potential values were then plotted against the current densities. The flow rates of the concentrate and the diluate were kept constant as 0.145 m/sec. All experiments were performed at 22~25°C.

2.2.2. The Dependence of Current-voltage Relation on the Concentration of the Concentrate

The NaCl concentration in the concentrate compart-

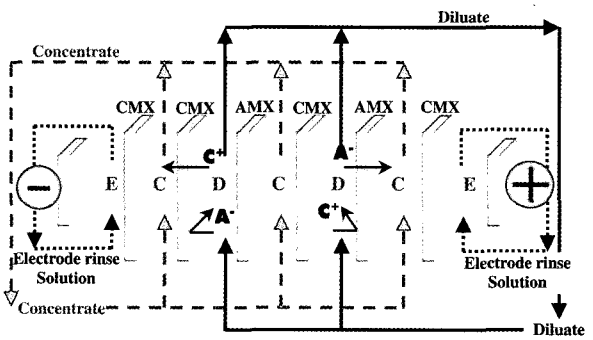

Fig. 1. Schematic diagram of the electrodialysis stack used for desalination of the brackish water (CMX: cation-exchange membrane, AMX: anion-exchange membrane, C: concentrate compartment, D: diluate compartment, E: electrode compartment, C^+: cations, A^-: anions).

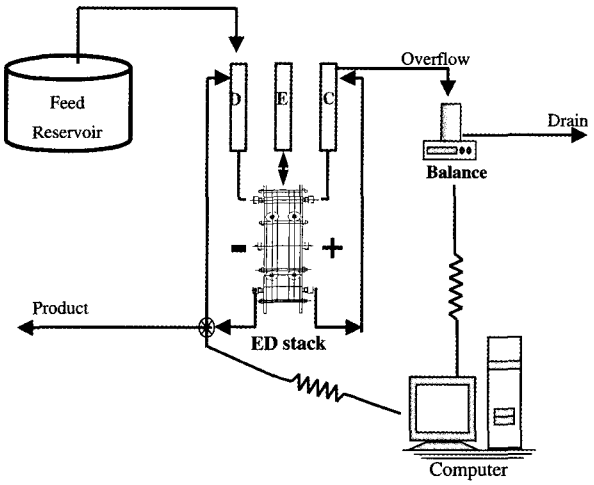

Fig. 2. Schematic diagram of the experimental set-up for desalination of the brackish water. D, E, and C stand for the diluate, electrolyte, and concentrate solutions, respectively.

ment was varied from 0.188 M to 4 M and that of the diluate was maintained as 0.188 M. Therefore, the diluate and concentrate solutions were circulated separately at a rate of 0.145 m/sec. The current-voltage relation was obtained for a very short time to minimize the change of concentration. The cell configuration, membrane area, and temperature were the same as those of the previous experiment while the current was increased by 0.5 A every five seconds and the potential was measured every second and averaged for each current step.

2.3. Desalination of Brackish Water

The desalination experiment was performed using the stack consisting of two cell pairs with both AMX and CMX membranes (Fig. 1). The AMX and CMX membranes were selected based on their high mechanical strength allowing for a long-term operation. The stack included seven compartments and the outer compartments contained electrodes, *i.e.*, a platinum anode and a stainless steel cathode. Alternating the AMX and CMX membranes separated the concentrate and the diluate compartments.

In this experiment, an automatic electrodialysis system was used for the observation of fouling caused by the inorganic materials in the brackish water. The experimental set up is shown in Fig. 2. Brackish water was used as the feed solution and initial concentrate solution and 0.5 M Na_2SO_4 solution was used as the electrode solution. The feed was replaced with 1 L of fresh brackish water automatically after it was desalted to the conductivity of 2 mS/cm, which meets the standard for drinking water. For the concentrate and electrode solutions, 1 L of each solution was prepared prior to the desalination experiment and was not replaced until the experiment was completed.

Although limiting current densities for the CMX and AMX membranes were 2,730 A/m^2 and 2,620 A/m^2, respectively, a low current density, 300 A/m^2, was supplied by a power supply (HP 66332A, USA), to prevent pH drop in the diluate compartment below the drinking water standard, 5.8. The desalination was performed under a constant current mode.

The overflowing concentrate solution was measured using a balance (Sartorius CP3202S, German). The pH and conductivity data of the feed solution were also monitored using pH meters (Model C2506, Broadley James, USA) and conductivity meters (Model con1000, Eutech, Singapore), respectively. The resistance for one cell pair in the stack was obtained using a multimeter (Model M4W-V, Autonics, Korea) connected to Pt wires. The product and the concentrate were sampled and their ion concentrations were analyzed by ion

chromatography (DX-500, ED 40 conductivity detector, CS 12A column, Dionex, USA).

2.4. Characterization of the CMX and AMX Membranes

The contact angle of each membrane, an index of the hydrophobicity, was measured using a contact angle meter (CAM-PLUS II, Tantec, USA). Before the measurement, membranes were dried for 48 hours. This experiment was repeated five times and the values were averaged.

The resistance of membranes was measured using FRA2 (Frequency response analyzer) linked to the potentiostat/galvanostat. An electrical current was supplied by a potentiostat/galvanostat (Model PGSTAT 30, AutoLab, Netherlands) connected to the counter electrode and working electrode plates (Ag/AgCl). The experiment was carried out at a frequency of 100 kHz.

The zeta potential of the membrane surface was obtained by measuring electrophoretic mobility of a standard particle, polystyrene latex (Diameter 52 nm, Otsuka Electronics, Japan) coated with HPC (MW 300,000, Scientific Polymer Products, Japan). For this experiment, a microelectrophoresis cell unit (ELS-600, Otsuka Electronics, Japan) was used. The dependence of the zeta potential on pH was also determined for the cation exchange membrane. Membrane surfaces were observed using a field-emission scanning electron microscope (FE-SEM, S-4700, Hitachi, Japan).

3. Results and Discussion

3.1. The Limiting Salt Concentration in the Concentrate During the Desalination of Brackish Water

The desalination process decreased the conductivity of brackish water to 2 mS/cm to meet the requirements of drinking water, while the conductivity of the concentrate continued to increase as shown in Fig. 3. Theconductivity of the concentrate approached to 170 mS/cm after treating 60 L ofbrackish water. At the same time, an abrupt drop in the temperature of the

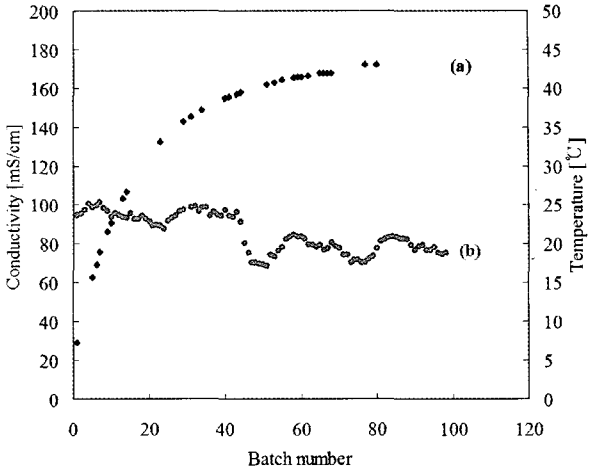

Fig. 3. Variations in the conductivity and the temperature of the concentrate; (a) the conductivity, (b) the temperature.

concentrate compartment was observed. This sudden change in the temperature is a result of $CaSO_4$ scale formation on the CMX membrane surface in the concentrate compartment. Once precipitation started to form, additional Ca^{2+} and SO_4^{2-} ions accumulated on the surface of the precipitate particles. Finally, the scales blocked flow channel and reduced the flow rate during the 40^{th} batch. With the decrease of flow rate, the temperature of the concentrate compartment dropped and the conductivity reached a steady state more rapidly.

Theoretically, as an operation proceeds, ion concentration within the concentrate compartment should increase linearly. However, the experimental data showed that the actual concentration did not increase linearly with time due to the water flux resulting from osmosis and electro-osmosis. That is, when ions are transported into the concentrate compartment they carry water molecules with them and it contributes to the dilution of the concentrate solution. The phenomena refer to the osmosis, which can be expressed by the following equation[20]:

$$\frac{dV}{dt} = \frac{\varepsilon I \zeta}{\eta \kappa} \quad (1)$$

where, dV/dt is the flow rate generated by electro-

osmosis, I is the current, κ is the electrical conductivity of the brackish water, ε is the permittivity of the solution or the dielectric constant, and η is the viscosity. If all variables are constant in the equation, the flow generated by electro-osmosis is constant. Additionally, water molecules also can move into the concentrate compartment by osmotic pressure due to concentration difference between the concentrate compartment and diluate compartment. However, the effect of osmosis can be neglected because ion-exchange membranes are non-porous. In this experiment, the flow rate generated by electro-osmosis only was 41.2 mL/hr.

Fig. 4 shows the variation in ion concentration of the concentrate and the diluate. The y-axis represents equivalent NaCl concentration calculated from the concentration of all the ions contained. The analyzed concentration in concentrate compartment was in accordance with the predicted value from the mass balance. After the 40th batch, the measured concentration deviated a little from the theoretical line. This deviation can be explained by the following differential equation:

$$V_C \frac{\partial C}{\partial t} = \frac{(C_{D,i} - C_{D,f})}{\tau} - C \cdot J_{over} \quad (2)$$

where V_C and C are the volume and the ion concentration in the concentrate, t is the time, τ is the average time required to desalt 1 L of brackish water, $C_{D,i}$ and $C_{D,f}$ are initial and final concentrations of the diluate, respectively, and J_{over} is the flux of overflow from the concentrate compartment or the electro-osmotic flux. The left-hand side of the equation corresponds to the rate of ion accumulation in the concentrate compartment, while the first term of the right-hand side refers to ion flux into the concentrate by desalination and the second is ion flux getting out of the concentrate due to an overflow. By integrating equation (2), we can obtain:

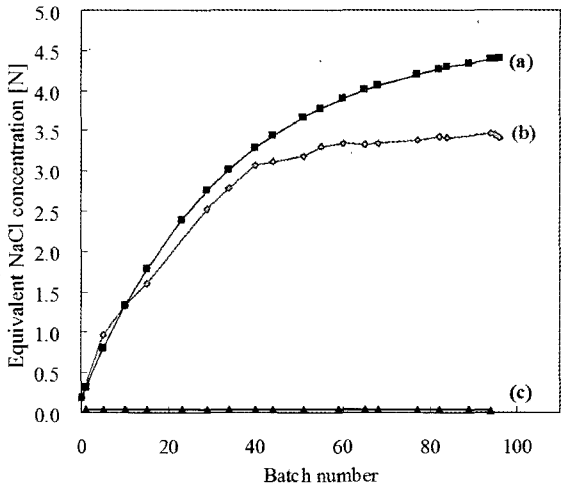

Fig. 4. Variation in the salt concentration of the concentrate and product; (a) the calculated salt concentration within the concentrate, (b) the actual concentration within the concentrate, (c) the measured salt concentration within the product.

$$C = \left(C_i \frac{C_{D,i} - C_{D,f}}{\tau \cdot J_{over}}\right) \cdot exp\left(-\frac{J_{over}}{V_C} t\right) - \frac{C_{D,i} - C_{D,f}}{\tau \cdot J_{over}} \quad (3)$$

where C_i is the initial concentration of the concentrate. The result of this equation is plotted in Fig. 4 for the comparison with the actual data. The calculated ion concentration increased up to 4.4 N NaCl - equivalence, and then reached a steady state, while the experimentally measured value remained at only 3.4 N. This deviation between the experimental data and the calculated value after the 40th batch was the result of precipitation of some salts in the concentrate compartment. The salt concentration of the product water was 0.014 M in average with a standard deviation of 0.0016 M.

3.2. Formation of $CaSO_4$ Scale on the CMX Membrane Surface

The Ca^{2+} and SO_4^{2-} ion concentrations in the concentrate for each batch were measured by ion chromatography. The index for the precipitation of gypsum is defined as[21]:

$$S = 1000(\sqrt{X^2 + 4K} - X) \quad (4)$$

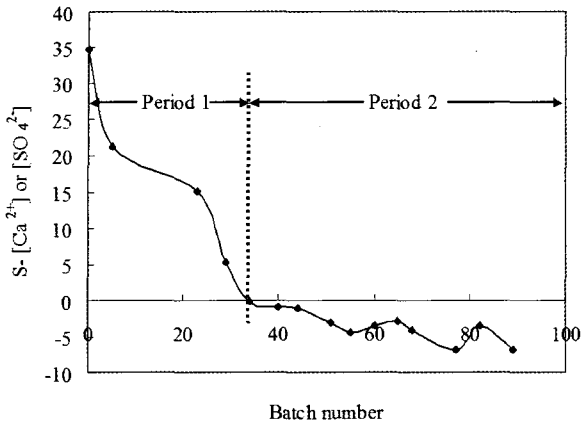

Fig. 5. Difference between S and the lower concentration of the two ions (Ca^{2+}, SO_4^{2-}) versus the batch number. Here S is $1000[\sqrt{\chi^2+4k}-x]$ where X is the difference between the Ca^{2+} and SO_4^{2-} concentrations.

where S is gypsum solubility in meq/L, X is the difference between Ca^{2+} and SO_4^{2-} concentrations, and K is a constant varying with ionic strength of a solution. The K values according to the ionic strength were taken from Nedelmann's data[21]. Fig. 5 shows the difference between the S value and the smaller among two concentrations of Ca^{2+} and SO_4^{2-} ions. Before the saturation concentration (period 1), calcium and sulfate ions were concentrated in the concentrate compartment without deposition yet. At the 34th batch, the difference changed from a positive to a negative value, indicating that gypsum started to precipitate. In the period 2, the ion concentration exceeded the solubility product constant of calcium sulfate and continued to increase. After the precipitation started, accumulation of $CaSO_4$ was progressed, and then the flow rate of the concentrate dropped during the 40th batch as mentioned previously.

Fig. 6 shows the SEM images of virgin and fouled CMX membrane surfaces with 20,000-fold magnification. The images show the aggregated particles are covering the fouled cation exchange membrane while no scaling material was observed on the AMX mem-

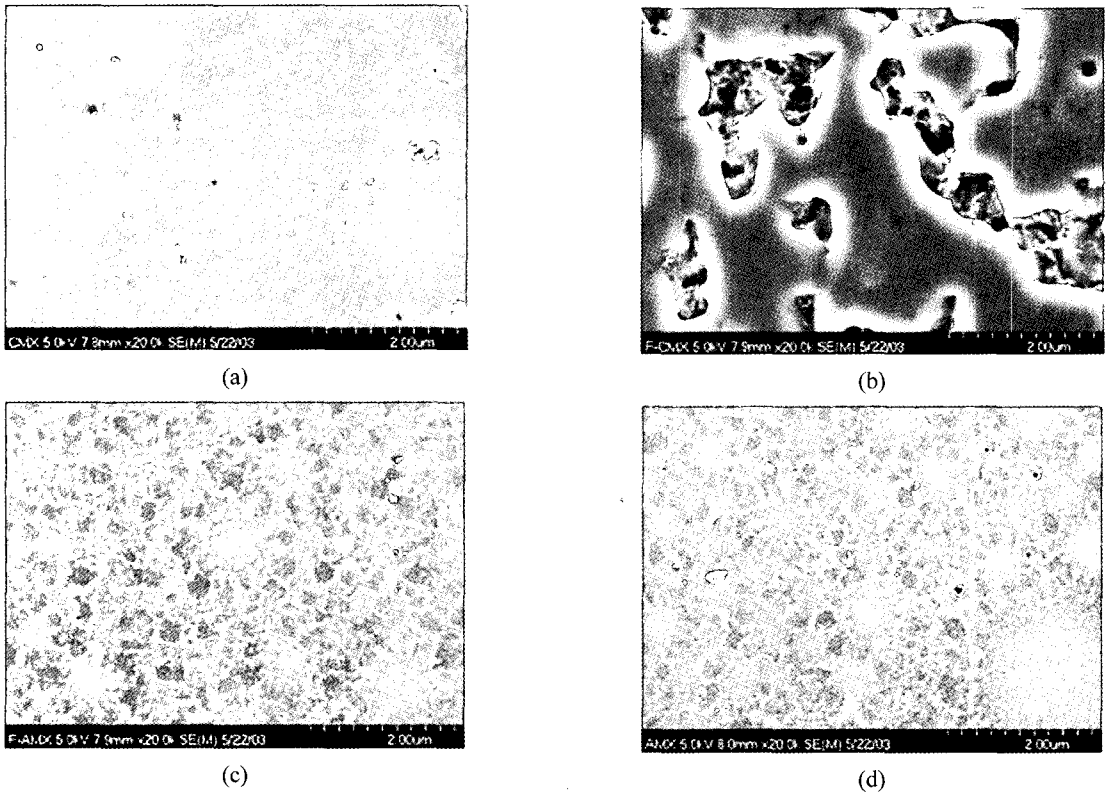

(a) (b) (c) (d)

Fig. 6. 20,000-fold magnification of the CMX and AMX membranes; (a) virgin CMX membrane, (b) fouled CMX membrane, (c) virgin AMX membrane, (d) fouled AMX membrane.

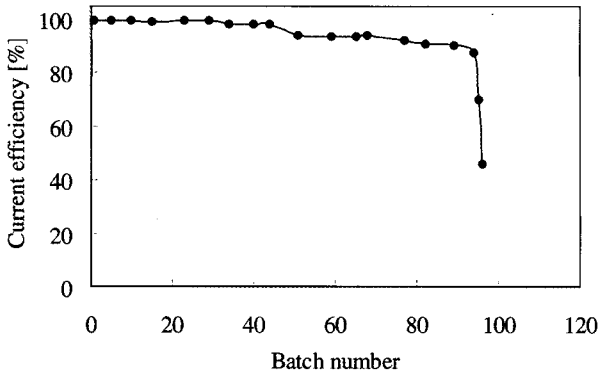

Fig. 7. Current efficiency versus the batch number.

brane surface.

3.3. Water Dissociation by Back Diffusion

This electrodialysis process was stopped during the 96th batch because the turbidity in the diluate compartment increased with the abrupt dropping of current efficiency. The current efficiency is shown in Fig. 7 as a function of batch number. The efficiency decreased to 46.3% during the last batch. The particles causing high turbidity were identified as $Mg(OH)_2$ by ionic analysis. In addition, the hydroxide concentration increased rapidly bringing the pH to 11.3 as a result of the water dissociation on the CMX membranes (Fig. 8). Considering that the solubility product constant of $Mg(OH)_2$ is 7.1×10^{-12} at 25°C, precipitation of that was evident. Although the limiting current densities in the experiment were higher than the operating current density as 2,730 A/m^2 and 2,620 A/m^2 for the CMX and AMX membranes respectively, water dissociation occurred due to decrease in the limiting current densities. Since $CaSO_4$ scales formed on the CMX membrane led to the change, the current-voltage relation of a fouled CMX membrane was compared with a virgin CMX membrane in Fig. 9. The ion concentrations within the diluate and the concentrate remained constant as 0.188 mol/L NaCl during the measurement of the limiting current density. As shown in the figure, the limiting current density dropped from 2,730 A/m^2 to 1,620 A/m^2 due to the $CaSO_4$ scales formed on the membrane surface. For the fouled CMX membrane, the

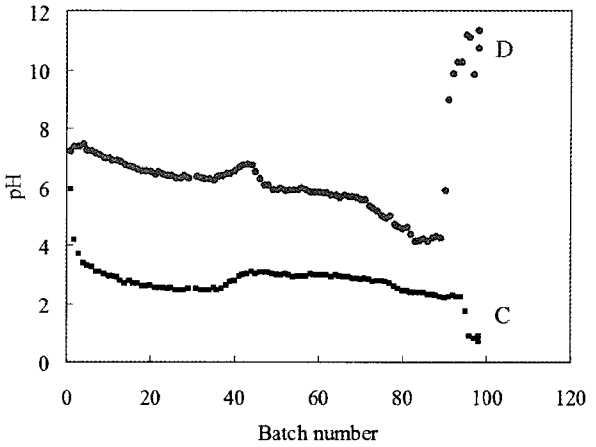

Fig. 8. Variations in the pH during the overall process time; C and D refer to the pH of the concentrate and the diluate respectively.

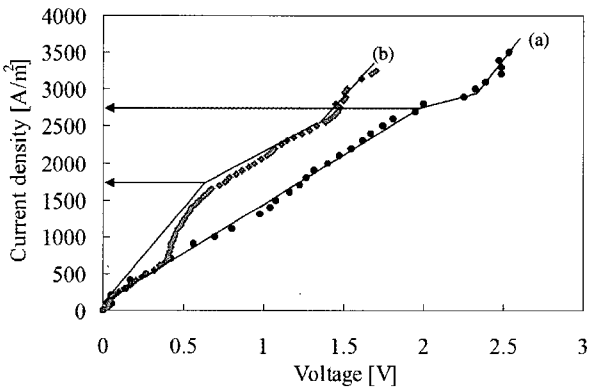

Fig. 9. Comparison between the current-voltage relations of a virginal and fouled CMX membrane; (a) virgin CMX membrane and (b) fouled CMX membrane.

plateau region was not evident in the plot of the current-voltage relation because of the non-homogeneity of the scale layer. The non-homogeneous surface made the resistance distribution irregular on the membrane surface and a part of the membrane surface reached the water dissociation potential even at a low current density.

In Fig. 10 variations in the limiting current density were observed while using solutions with different salt concentrations. Generally, the limiting current density is expressed by the Nernst-Planck equation for the ionic concentrations within the diluate compartment without influence of the concentrate solution. During

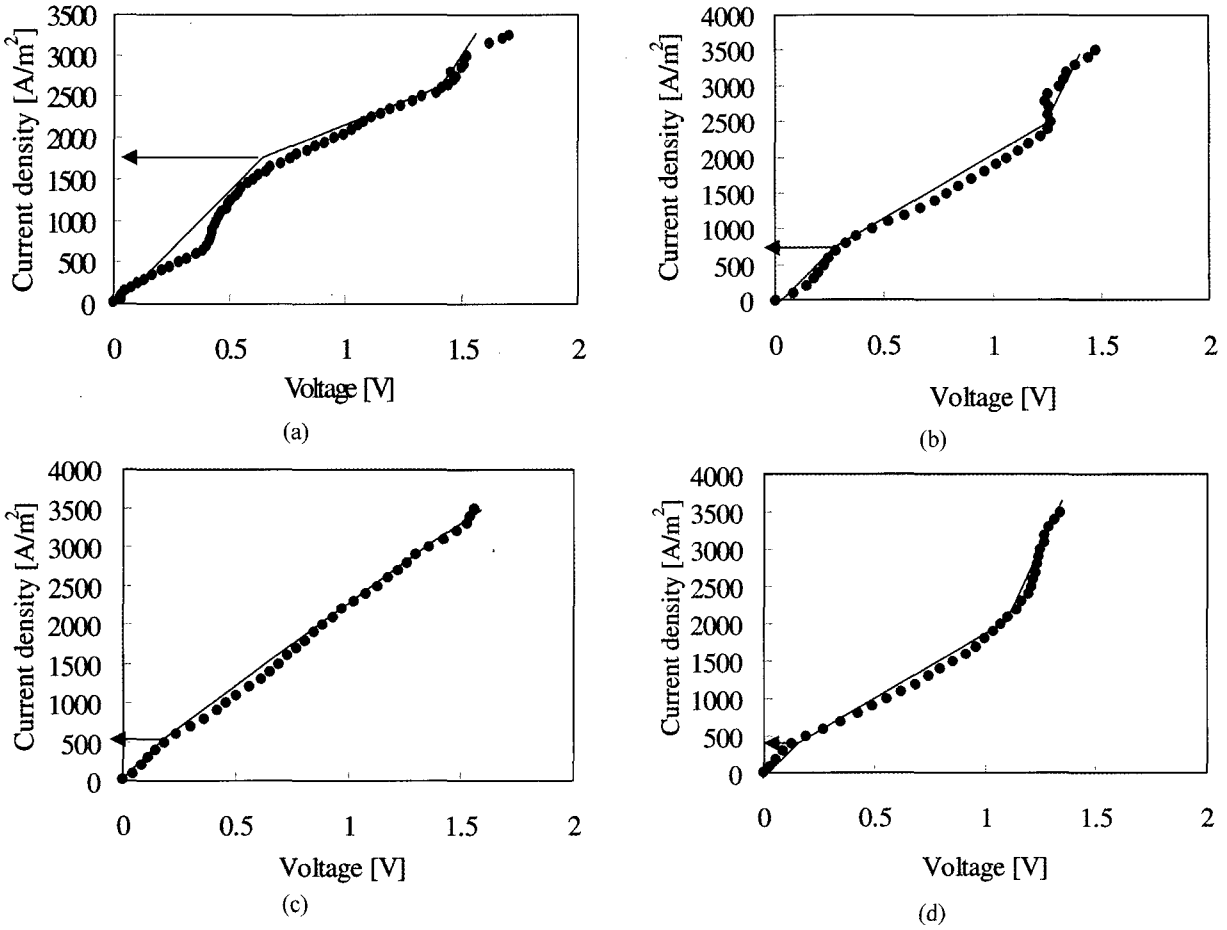

Fig. 10. Current-voltage relation for a fouled CMX membrane according to the salt concentration within the concentrate compartment; The NaCl concentrations were (a) 0.188 mol/L, (b) 1.00 mol/L, (c) 3.00 mol/L, (d) 4.00 mol/L. The concentrations within the diluate were all 0.188 mol/L.

the brackish water desalination experiments, diluate was refreshed by brackish water every batch while the salt in the concentrate accumulated continuously. Therefore, the difference in ion concentrations between the two compartments increased with time. Such a condition might affect the limiting current density. In Fig. 10, the diluate concentration was constant as 0.188 mol/L NaCl and the concentrate concentration was variable (0.188, 1.00, 3.00 and 4.00 mol/L NaCl). The limiting current densities for each concentrate concentration are listed in Table 1. It is noteworthy that when the ion concentration of the concentrate was 4.00 mol/L, the limiting current density was the same as the experimental operating current density and, consequently, water dissociation was observed.

Table 1. Limiting Current Densities for Virgin and Fouled CMX Membranes According to the NaCl Concentration Within the Concentrate

Membranes	Concentration of concentrate (mol/L)	Limiting current density (A/m^2)
Virgin CMX membrane	0.188	2,730
Fouled CMX membrane	0.188	162
	1.00	80
	3.00	60
	4.00	30

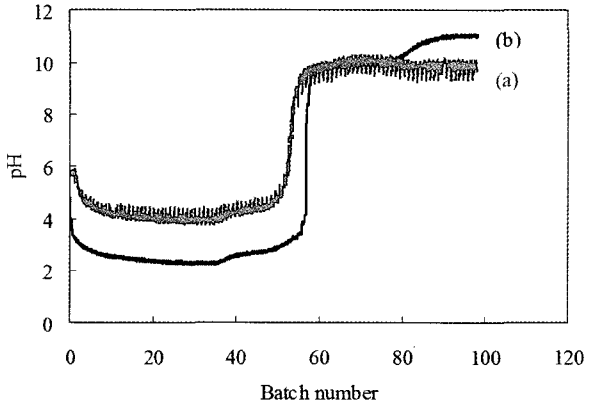

Fig. 11. Variations of the pH versus the batch number during the desalination of a NaCl solution; (a) and (b) are for the diluate and the concentrate, respectively.

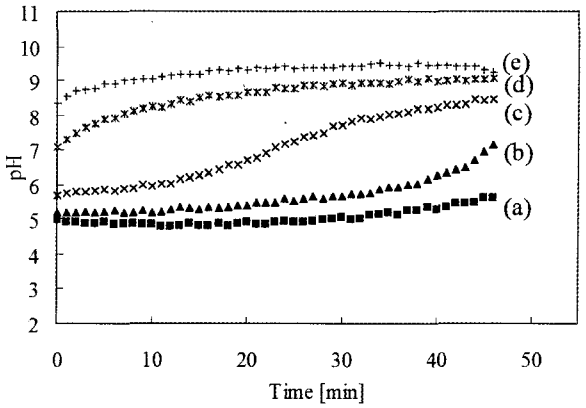

Fig. 12. Variations in the diluate from 52nd batch to 56th batch in figure 11; (a) 52nd batch, (b) 53rd batch, (c) 54th batch, (d) 55th batch, (e) 56th batch.

3.4. Desalination of NaCl Solution with the Same Concentration as Brackish Water

Because of water dissociation, the pH of diluate compartment increased to 11.3, $Mg(OH)_2$ precipitate was formed and the current efficiency dropped abruptly. To further investigate the phenomena occurring after water dissociation, we used a 0.188 M equivalent NaCl solution as feed instead of the brackish water. Fig. 11 shows the pH variation versus batch number during the desalination of NaCl solution. The pH of the diluate began to increase sharply, to about 10 at the 53rd batch, and then, that of the concentrate also increased at the 80th batch.

From these results, it can be said that water dissociation occurred on the surface of the CMX membrane around the 53rd batch, and the AMX membrane at about the 80th batch. Although both of CMX and AMX membranes were not fouled, water dissociation was shown at an earlier batch than when the brackish water was used. The reason for this is that the concentration difference between the concentrate and the diluate became greater even for a shorter operation time since the magnesium and sulfate ions did not accumulate in the concentrate compartment and did not block the concentrate channel. The greater concentration difference accelerated the water dissociation. Fig. 12 shows the change of pH within the diluate compartment from the 52nd batch to 56th batch in detail. In the 52nd batch, no water dissociation was observed while pH began to increase at the end of the 53rd batch. The time required for the pH to increase was shortened as the batch number went further. According to the Nernst-Planck equation, the limiting current density was determined when the ion concentration at the membrane surface was zero and the concentration gradient could not increase any longer. However, in this experiment, the water dissociation was observed before the surface concentration reached zero.

This phenomenon can be explained by the back diffusion through CMX membrane. As the concentrate was further concentrated, the concentration gradient between diluate and concentrate became larger and caused the back diffusion of ions. In the Nernst-Planck equation, it is assumed that the transport of the ions in the membrane is much faster than that in the boundary layer. However, the higher concentration gradient can prevent ions from moving through the membrane due to the back diffusion. Furthermore, at any moment, transport through the membrane may be more difficult than in the boundary layer and, thus, be the rate determining step. Therefore, although the membrane suface concentration is not zero, water dissociation can take place above the limiting current density.

Water dissociation was seen on AMX membranes also at the 80th batch. This suggests that the limiting current density of the AMX membrane decreased from

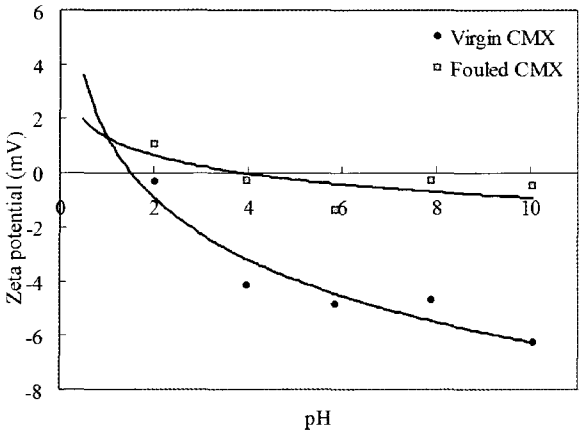

Fig. 13. Zeta-potential of the virgin and the fouled CMX membranes as a function of pH.

the initial limiting current density of 2,620 A/m^2 to the process current density of 300 A/m^2.

Therefore it was thought that the water dissociation observed during the desalination of the sodium chloride solution and the brackish water was mainly caused by the back diffution caused due to a large concentration gradient and the formation of $CaSO_4$ scales, respectively.

3.5. Comparison of the Virgin and Fouled CMX Membranes and Their Characteristics

Changes in the properties between the virgin and fouled membranes were observed using several characteristics of membranes: zeta potential, impedance spectroscopy, contact angle, water content ratio, and ion exchange capacity. Fig. 13 shows the variation in the zeta potential of the virgin and fouled CMX membranes. While the virgin CMX membrane had the isoelectric point of 1.52 and the effect of pH on the zeta potential was distinct, the isoelectric point of fouled CMX membrane was higher, *i.e.*, 3.86, and the influence of the pH was insignificant. The surface of fouled CMX membrane was covered with $CaSO_4$ scale layer, and this exhibited a weak acidic characteristic because it was a salt from a weak base, $Ca(OH)_2$ and a strong acid, H_2SO_4. Therefore, the isoelectric point of the fouled membrane was slightly inclined toward acid as 3.86. Since there is no actual proton in the calcium sulfate molecule, its zeta potential was nearly independent of the pH. On the other hand, the sulfonic group on the virgin CMX membrane is very strongly dissociated and the pKa of sulfonic acid is as low as 1.77, which explains the low isoelectric point of the virgin membrane.

Table 2. Characterization of Virgin and Fouled CMX and AMX Membranes

Characterization	CMX		AMX	
	Virgin	Fouled	Virgin	Fouled
Resistance [Ω · cm^2]	3.15	3.00	2.92	3.04
Water content ratio	0.254	0.338	0.257	0.261
Ion exchange capacity [meq/g]	1.59	1.62	1.70	1.51
Contact angle [°C]	62.9	48.2	83.6	84.2
Thickness [mm]	0.157	0.217	0.137	0.143

The resistance of the CMX membrane decreased slightly after it was fouled (Table 2), while the water content, ion exchange capacity, and membrane thickness increased slightly. Although the membrane was fouled with a $CaSO_4$ scale layer, its main properties did not change significantly and the fouling itself did not affect the process efficiency. Only the limiting current density decreased significantly. Furthermore, the limiting current density decreased to a greater extent with the higher concentration gradients. Therefore, water dissociation occurred and $Mg(OH)_2$ precipitate was formed in the diluate compartment followed by an abrupt drop in the current efficiency. Also, the characteristics and performance of the AMX membrane did not show any significant changes as shown in Table 2.

4. Conclusions

In this study, we investigated the fouling mechanism of electrodialysis in terms of the limiting salt concentration within the concentrate during the desalination of brackish water. Also, the scale layer that formed on the CMX membrane surface itself did not have an effect on the process efficiency. The resistance of the

membrane even decreased a little. Only the limiting current density of the fouled CMX membrane was significantly lower than that of the virgin membrane. The limiting current density was further lowered by the increasing concentration difference between the diluate and the concentrate. Therefore it is recommended that the electrodialysis be operated under the limiting concentration of the concentrate compartment. Furthermore, it should be noted that the Nernst-Planck equation cannot fully explain the ion transfer phenomena in electrodialysis when the concentrate compartment is filled with a strong solution.

Acknowledgement

This work was supported in part by a grant from Sustainable Water Resource Research Center (SWRRC) through the Water Reuse Technology Center (WRTC) in Gwangju Institute of Science and Technology (GIST), and in part by the Brain Korea 21 from the Ministry of Education through the Chemical and Environmental Engineering program at GIST.

References

1. W. S. Winston, H. Kamalesh, and K. Sirkar, "Membrane Handbook," Van Nostrand Reinhold Publ., New York (1992).
2. K. H. Yeon and S. H. Moon, "Principle and Application of Continuous Electrodeionization," *Membrane Journal*, **11**, 61 (2001).
3. B. K. Park, B. P. Hong, K. S. Yeo, M. H. Yun, H. S. Byun, and H. J. Kang, "Preparation and Application of Pore-filled PVDF Ion Exchange Membrane," *Membrane Journal*, **14**, 108 (2004).
4. J. P. van der Hoek and J. A. M. H. Hofman, "Electrodialysis as an alternative for reverse osmosis in an integrated membrane system," *Desalination,* **117**, 159 (1998).
5. Y. Tanaka, "Water dissociation in ion-exchange membrane electrodialysis," *J. Membr. Sci.*, **203**, 227 (2002).
6. M. Turek, "Cost effective electrodialytic seawater desalination," *Desalination*, **153**, 371 (2002).
7. J. M. Ortiz, J. A. Sotoca, E. Expósito, F. Gallud, V. García-García, V. Montiel, and A. Aldaz, "Brackish water desalination by electrodialysis: batch recirculation operation modeling," *J. Membr. Sci.*, **252**, 65 (2005).
8. P. Tsiakis and L. G. Papageorgiou, "Optimal design of an electrodialysis brackish water desalination plant," *Desalination,* **173**, 173 (2005).
9. E. Korngold, L. Aronov, N. Belayev, and K. Kock, "Electrodialysis with brine solutions oversaturated with calcium sulfate," *Desalination*, **172**, 63 (2005).
10. N. Kahraman, Y. A. Cengel, B. Wood, and Y. Cerci, "Energy analysis of a combined RO, NF, and EDR desalination plant," *Desalination,* **171**, 217 (2005).
11. H. J. Lee and S. H. Moon, "Fouling of Ion Exchange Membranes and Their Fouling Mitigation," *Membrane Journal*, **12**, 55 (2002).
12. J. H. Choi and S. H. Moon, "Concentration Polarization Phenomena in Ion-Exchange Membranes," *Membrane Journal*, **12**, 143 (2002).
13. J. S. Park, J. H. Choi, and S. H. Moon, "Operation of Electrodialysis at Over Limiting Current Density," *Membrane Journal*, **12**, 171 (2002).
14. M. S. Kang, Y. J. Choi, and S. H. Moon, "Effects of Immobilized Bipolar Interface Formed by Multivalent and Large Molecular Ions on Electrodialytic Water Splitting at Cation-Exchange Membrane Surface," *Membrane Journal*, **13**, 143 (2003).
15. V. I. Zabolotsky, V. V. Nikonenko, and N. D. Pismenskaya, and A. G. Istoshin, "Electrodialysis technology for deep demineralization of surface and ground water," *Desalination*, **108**, 179 (1996).
16. E. James Watkins and Peter H. Pfromm, "Capacitance spectroscopy to characterize organic fouling of electrodialysis membranes," *J. Membr. Sci.*, **162**, 213 (1999).

17. Y. Tanaka, "Mass transport and energy consumption in ion-exchange membrane electrodialysis of seawater," *J. Membr. Sci.*, **215**, 265 (2003).
18. I. Atamanenko, A. Kryvoruchko, L. Yurlova, and E. Tsapiuk, "Study of the $CaSO_4$ deposits in the presence of scale inhibitors," *Desalination*, **147**, 257 (2002).
19. Tokuyama Soda Inc., "Neosepta ion exchange membranes," Product brochure, Japan, (1995).
20. M. Mulder, "Basic Principles of Membrane Technology," Kluwer Academic Publishers, Dordrecht Boston, London (1996).
21. H. G. Heitmann, "Saline water processing," pp. 45 VCH Press, New York (1990).